THE JOURNAL OF PHYSICAL CHEMISTRY B

ARTICLE

pubs.acs.org/JPCB

Velocity Effect on Aptamer-Based Circulating Tumor Cell Isolation in Microfluidic Devices

Yuan Wan,[†,‡] Jifu Tan,[§] Waseem Asghar,[‡,∥] Young-tae Kim,[†,‡] Yaling Liu,[§] and Samir M. Iqbal[*,‡,∥,⊥]

[†]Department of Bioengineering, University of Texas at Arlington, Arlington, Texas 76010, United States

[‡]Nanotechnology Research and Teaching Facility, University of Texas at Arlington, Arlington, Texas 76019, United States

[§]Department of Mechanical Engineering and Mechanics, Bioengineering Program, Lehigh University, Bethlehem, Pennsylvania 18015, United States

[∥]Department of Electrical Engineering, University of Texas at Arlington, Arlington, Texas 76011, United States

[⊥]Joint Graduate Committee of Bioengineering Program, University of Texas at Arlington and University of Texas Southwestern Medical Center at Dallas, University of Texas at Arlington, Arlington, Texas 76010, United States

ABSTRACT: The isolation and detection of rare circulating tumor cells (CTCs) has been one of the focuses of intense research recently. In a microfluidic device, a number of factors can influence the enrichment capability of surface-bound probe molecules. This article analyzes the important factor of flow velocity in a microfluidic channel. The competition of surface-grafted anti-EGFR aptamers to bind the overexpressed EGFR on cell membranes against the drag force from the fluid flow is an important efficiency determining factor. The flow rate variations are applied both in experiments and in simulation models to study their effects on CTC capture efficiency. A mixture of mononuclear cells and human Glioblastoma cells is used to isolate cancer cells from the cellular flow. The results show interdependence between the adhesion probability, isolation efficiency, and flow rate. This work can help in designing flow-through lab-on-chip devices that use surface-bound probe affinities against overexpressed biomarkers for cell isolation. This work demonstrates that microfluidic based approaches have strong potential applications in CTC detection and isolation.

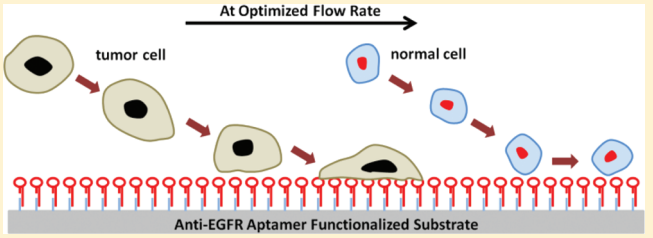

INTRODUCTION

The isolation and detection of rare circulating tumor cells (CTCs) is critical to establish cancer prognosis, design personalized therapy, and disease monitoring. Enumeration of CTCs, when these are very rare, can be potentially used as an indicator of a developing tumor.[1,2] A number of approaches have been reported for the direct or indirect detection of CTCs.[3−8] In these strategies, antibody-based cancer cell isolation has been widely adopted because affinity interaction-based cell sorting methods can yield higher efficiency and greater specificity.[9] With optimized chip pattern design and fluid flow parameters, CTCs can be directly isolated from patients' whole blood in antibody functionalized microfluidic devices.[10,11] However, high levels of off-target cross-reactivity[12] and need for conditions to retain probe protein functionality are major disadvantages of antibody-based approaches. Aptamers, as novel recognition elements, have been shown to have considerable affinities and higher specificities, comparable to those of antibodies.[13] They can be chemically synthesized, site-specifically labeled, and site-specifically immobilized. Aptamers have been used in cell labeling studies,[14,15] activating cell signaling pathways,[16,17] and cell isolation.[18]

Epidermal growth factor receptor (EGFR) is the most frequently overexpressed receptor tyrosine kinase (RTK) oncogene in all human malignancies. EGFR is activated upon binding to various growth factors and, consequently, initiates a signal transduction cascade that promotes cell migration, adhesion, invasion, cell proliferation, angiogenesis, and antiapoptosis.[19] It is thus an attractive target for cancer therapy,[20,21] and the expression levels of EGFR in cancer cells can be over 100 times higher than those in normal cells.[22,23] It has been reported that primary human glioblastoma (hGBM) cells, overexpressing EGFR, can be captured on anti-EGFR aptamer-functionalized glass substrates.[24] A mixture of hGBM and fibroblast cells in PBS were incubated with anti-EGFR aptamer-modified glass substrates, and hGBM cells were specifically enriched. Elution of cells to remove normal cells and nonspecifically bound tumor cells is often a subjective parameter in such studies.[25] The binding between aptamers and EGFR depends on their respective density and amount; if the sizes of normal cells in a cell mixture are relatively homogeneous, there can be a specific washing speed to elute most of them. However, it is well-known that the white blood cells (WBC) in peripheral blood have various sizes, with diameters ranging between 8 and 20 μm.[26] The variations in size indirectly result in the differential adhesion force. Because of the huge

Received: June 13, 2011
Revised: October 25, 2011
Published: October 26, 2011

Table 1. Parameters Used in the Calculation

	diameter (μm)	bond length (nm)	viscosity (pa s)	receptor density (#/m^2)
hGBM	10	10	1×10^{-3}	1×10^{15}
WBCs	10	10	1×10^{-3}	1×10^{14}

difference in the number of WBCs and CTCs, without reasonable washing speed, a large number of WBC can still remain on the surface and may further disturb the tumor cell genotype analysis. Moreover, the traditional tumor cell isolation methods cannot satisfy microanalysis, and therefore, microfluidic devices are required. Even if the eluting speeds are calculated based on the established models,[27−29] the value might not adapt to the dimensions of microfluidic devices. If tumor cells could be enriched with an optimized flow speed, the ratio of tumor cells during the capture process can be significantly increased. It is necessary to investigate the flow velocity effect on selective capture efficiency between tumor and normal cells in microfluidic devices. In this article, we first use a model to roughly estimate the adhesion probabilities of hGBM cells and bovine WBCs and then use a straight channel with 25 μm height to optimize the cell suspension flow speed. The results show that 1.5−2 mm/s might be the optimum flow rate that could be used for separating hGBM cells from WBCs.

EXPERIMENTAL METHODS

All chemicals were obtained from Sigma-Aldrich (St. Louis, MO) unless otherwise noted.

Computational Model of Cell Capture. Numerical simulations have been widely used to study the binding probabilities of nanoparticles and cells.[29−31] In this article, a computational model is developed to determine the range of optimal velocities under which the captured hGBM cells can be kept on the anti-EGFR aptamer functionalized surface while as many WBCs are eluted as possible. Cells are treated as rigid spherical objects since the focus is the magnitude of the cell adhesion force on a flat surface. The parameters used in the calculation are listed in Table 1. The main difference between the hGBM cell model and the WBC model is the surface receptor density. The hGBM cells have more receptors on the surface, thus require a larger flow rate to be detached.

The microchannel was designed with a 25 μm height and 1 mm width, where the flow was laminar. Newtonian flow was assumed for the fluid. Derived from Navier−Stokes equations, the fully developed velocity profile is given as

$$V_x = \frac{\Delta p h^2}{8\mu L}\left(1 - \frac{4y^2}{h^2}\right) \quad (1)$$

where Δp is the pressure difference, h is the channel height, L is the channel length, and μ is the viscosity of the fluid. A schematic velocity profile of the microchannel and hydrodynamic force applied to cells under shear flow is shown in Figure 1. The cells were adhered to the bottom of the microchannel. Hydrodynamic forces, especially the drag force F and the torque M, which would rotate and dislodge the cells, are required to remove the cells. The drag force and the torque are given by $F = 6\pi a l \mu S F^S$ and $M = 6\pi a^3 \mu S T^S$ where a is the radius of the cell, l is the separation

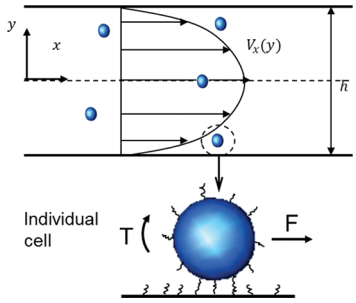

Figure 1. Schematic illustration of parabolic flow velocity profile and hydrodynamic force applied to cells under shear flow.

distance to the wall, μ is the viscosity of the fluid, S is the shear rate at the wall, and F^s and T^s are shape-dependent coefficients. Thus, the binding probability of the cell is given by

$$\frac{P_a}{m_r m_l K_a^0} = A_c \exp\left[-\frac{\lambda}{k_B T}\frac{F_{dis}}{m_r A_c}\right] \quad (2)$$

where m_r and m_l are the receptor and ligand densities, respectively; K_a^0 is the association constant at zero load of the ligand−receptor pair; A_c is the contact area; λ is the characteristic length of the ligand−receptor bonds; k_B is the Boltzmann constant; F_{dis} is the dislodging force acting per unit ligand−receptor pair; and T is the temperature (Figure 1).[25−27,30]

Aptamer Preparation. The aptamers were prepared as described before.[24] Briefly, the purified human EGFR protein (R&D systems, Minneapolis, MN) was used for preparing anti-EGFR RNA aptamer. It was purified from murine myeloma cells and contained the extracellular domain of human EGFR (Leu25-Ser645). The sequences for the anti-EGFR aptamer and DNA probe were: anti-EGFR aptamer (5′-GGC GCU CCG ACC UUA GUC UCU GUG CCG CUA UAA UGC ACG GAU UUA AUC GCC GUA GAA AAG CAU GUC AAA GCC GGA ACC GUG UAG CAC AGC AGA GAA UUA AAU GCC CGC CAU GAC CAG-3′); DNA probe (5′-amine-CTG GTC ATG GCG GGC ATT TAA TTC-3′). The anti-EGFR aptamer (K_d = 2.4 nM) was extended with a linker (underlined). The linker did not disrupt the aptamer structure but was used for hybridization with a DNA probe. The anti-EGFR aptamer was prepared by transcribing a double-stranded (ds) DNA template using Durascribe kits (Epicenter Biotechnologies, Madison, WI). The dsDNA template was PCR-amplified, ethanol precipitated, and mixed with reaction buffer, DTT, ATP, GTP, 2′ F-CTP, 2′ F-UTP, and a mutant T7 polymerase for 10 h at 37 °C. The DNA template was then degraded with DNase treatment for 30 min at 37 °C. The aptamer was purified on an 8% denaturing PAGE. The band for the aptamer was visualized by UV shadowing, and the aptamer was excised and eluted in 0.3 M NaAc (pH 5.2) overnight at 37 °C followed by ethanol precipitation. The pellet was dissolved in water, and the concentration of the aptamer was measured on a NanoDrop (Thermo Scientific, Wilmington, DE).

Microfluidic Channel Preparation. The channel was designed in AutoCAD. To obtain a thickness of 25 μm, SU8-25 photoresist was spin-coated at 500 rpm for 5 s followed by 2000 rpm for 25 s. The coated substrate was prebaked at 65 °C for 3 min and then soft-baked at 95 °C for 7 min. The 300 mJ/cm^2 energy was adopted for lithography exposure. The post bake was carried at 65 °C for 1 min and at 95 °C for 3 min. Finally, the master was gently rinsed first with pure developer solution and

then with isopropanol. Polydimethylsiloxane (PDMS) was mixed (10:1, wt/wt) with Sylgard 184 silicone elastomer curing agent (Dow Corning). The mixture was first placed in a vacuum chamber to remove all bubbles. PDMS devices were fabricated by casting PDMS solution on the SU8 master and curing on the hot plate at 150 °C for 5 min. Polymerized PDMS was gently peeled off the master. Sample reservoirs were prepared in the PDMS by punching 2 mm diameter holes with a steel rod.

Functionalizing Glass Substrates with Anti-EGFR Aptamers. The attachment protocol was adapted from earlier descriptions.[24,32] The 25 × 75 mm glass slides were cleaned with piranha solution (H_2O_2/H_2SO_4 in a 1:3 ratio) for 10 min. After rinsing with deionized water (DI water) and drying in nitrogen flow, glass slides were immersed in 3-aminopropyltriethoxysilane (APTES), prepared at 2% (v/v) in methanol, for 30 min at room temperature. The silanized slides were then sequentially rinsed with methanol and DI water and cured at 120 °C for 30 min. The substrates were then immersed in a dimethylformamide (DMF) solution containing 10% pyridine and 1 mM 1,4-phenylene diisothiocyanate (PDITC) for 2 h. Each substrate was then washed sequentially with DMF and 1,2-dichloroethane and dried under a stream of nitrogen.

A 200 μL volume of 30 μM DNA and RNA in 10 mM Tris, 1 mM EDTA, and 100 mM NaCl (pH 8) was heated up to 95 °C for 5 min and cooled gradually to room temperature. During the annealing process, probe DNA was hybridized with the linker part of RNA. The solution was incubated on glass substrates in a humidity chamber at 37 °C overnight. It is interesting to note here that the single-stranded probe DNA with an amine end group was complementary to the linker part of the RNA, and thus, this duplex was used to attach the aptamer to the surface via the amine end of the probe DNA. The RNA could have been modified with an amine directly, but it is much harder to modify RNA directly with an amine group while maintaining high synthesis yield. The RNA aptamer was thus elongated with the linker part and the complementary probe DNA with amine modification anchored it on the surface.

Each slide was then washed with diethylpyrocarbonate (DEPC) treated DI water (0.02% v/v). The unreacted PDITC moieties were deactived by 50 mM 6-amino-1-hexanol and 150 mM *N*, *N*-diisopropylethylamine (DIPEA) in DMF for 30 min at 37 °C. Each slide was then sequentially rinsed with methanol and DEPC-treated DI water. The PDMS cap was treated with UV Ozone plasma for 25 min and attached on the glass slide surface. Finally, the channel was filled with 1× (pH 7.5) phosphate buffered saline (PBS) with 5 mM magnesium chloride.

Human Glioblastoma (hGBM) Cells Culture. Cells were suspended in a chemically defined serum-free Dulbecco's modified Eagle's medium (DMEM)/F-12 medium, consisting of 20 ng/mL of mouse EGF (Peprotech, Rocky Hill, NJ, USA), 20 ng/mL of bFGF (Peprotech, Rocky Hill, NJ, USA), 1× B27 supplement (Invitrogen, Carlsbad, CA, USA), 1× insulin-transferrin-selenium-X (Invitrogen, Carlsbad, CA, USA), 100 units/mL: 100 μg/mL of penicillin/streptomycin (HyClone, Wilmington, DE, USA), and plated at a density of 3×10^6 live cells/60 mm plate. The hGBM cells were also stably transduced with a lentivirus expressing an *m-cherry* fluorescent protein.

Bovine Mononuclear Cells Preparation. Ten milliliters of bovine whole blood was mixed with 1.25 mL of OptiPrep (Axis-Shield, Norway), and 0.5 mL of tricine buffered saline (TBS) was carefully loaded on the top. The mixture was spun down at 2000*g* for 15 min. Mononuclear cells (i.e., WBCs) were collected from the top layer and resuspended in PBS. Mononuclear cells were washed three times with PBS to completely remove blood platelets. Cells were counted, and the density was recorded.

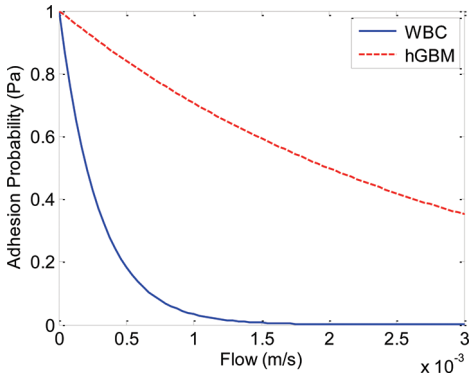

Figure 2. Adhesion probability of 7.5 μm diameter WBCs (blue solid line) and 12.2 μm diameter hGBM cells (red dashed line) on the anti-EGFR aptamer-functionalized surface at different flow rates.

Cells Captured with Microfluidic Device. After measuring cell density, the cell suspension was injected into the aptamer functionalized channel with different velocities: 0.5, 1, 1.5, and 2 mm/s (WBCs) and 1, 2, 4, and 6 mm/s (hGBM cells) for 10 min, and then 1× PBS was used to wash off the nonspecifically bound cells. Images were taken with a Leica DM Inverted microscope.

RESULTS AND DISCUSSION

Computation Results for Cell Capture Efficiency. Before the experiments, the sizes of hGBM cells and bovine peripheral blood mononuclear cells were measured (data not shown). The average diameter of hGBM cells was 12.2 μm (SD: 2.31). The isolated bovine mononuclear cells included monocytes and lymphocytes, and lymphocytes made up 90% of the samples. The average diameter of lymphocytes was 7.54 μm (SD: 0.63), a little smaller than hGBM cells. For facilitating computation, we used 7.5 μm as their diameter. From eq 2, the adhesion probability at different flow rates for WBCs and hGBM cells is plotted in Figure 2.

The adhesion probability for both WBCs and hGBM cells decreases as the flow rate increases. Comparing the adhesion probability, it shows that if more than 50% of the WBCs can be eluted while at least 50% of the hGBM cells are kept on the surface, the flow rate should be within 0.2 to 2 mm/s. At the flow rate of 1 mm/s, 68% of the hGBM cells are adhered to the surface compared to less than 2% of the WBCs. Thus, the computational model provides a guide for the choice of proper flow rate for the experimental setup.

Experimental Velocity Effect on Cell Capture. In a scenario of clinical diagnosis where isolated CTCs may be used as treatment indicators, the EGFR genotype of a tumor cell can be detected via PCR for guiding the chemotherapy and for monitoring its genotype change.[33] There it is necessary to collect as many CTCs as possible, while mitigating the collection of WBCs. Since WBCs carry a normal genotype, if a large amount of WBCs mingle with isolated CTCs, it will decrease the sensitivity of PCR. In this computation part, we utilized the property of tumor cells' EGFR overexpression on the cellular membrane to separate tumor cells from WBCs.

It is known that the concentration of immobilized aptamers can affect the cell isolation efficacy.[18] The higher the concentration

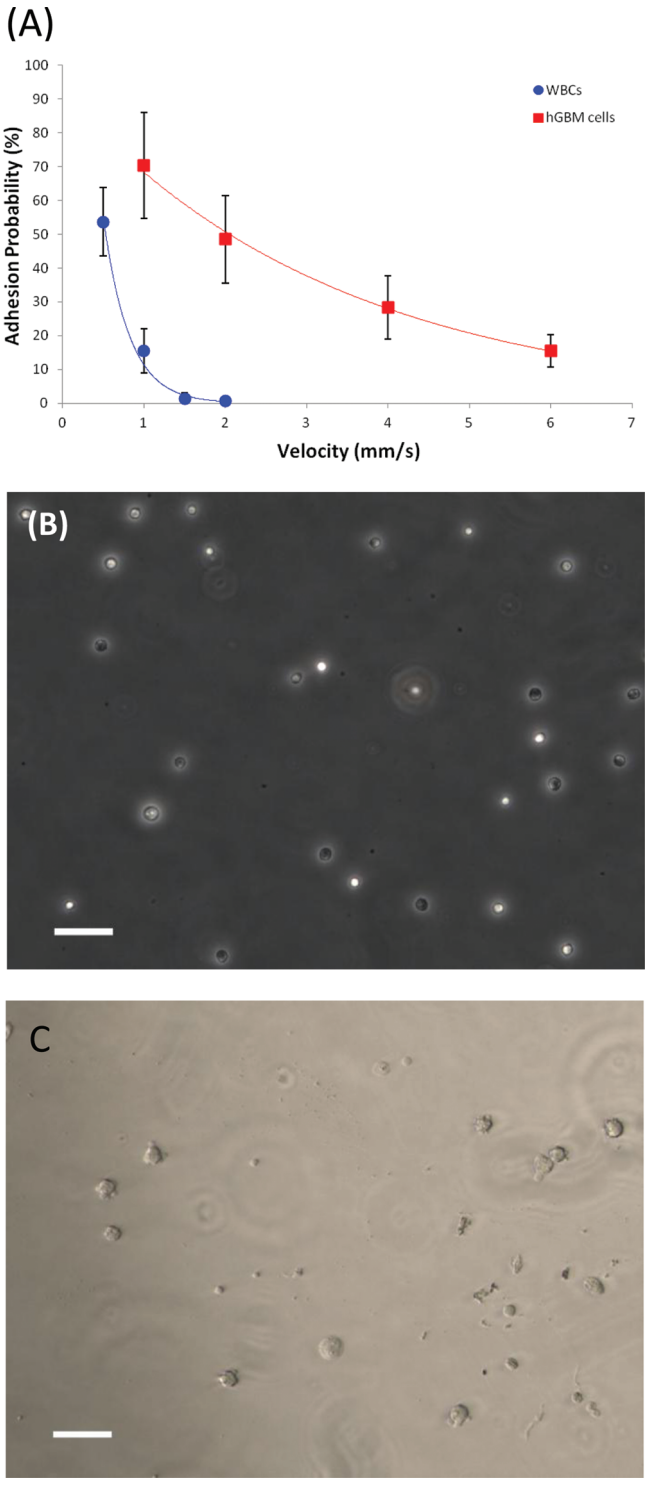

Figure 3. Experimental results of cells captured on the anti-EGFR aptamer-functionalized surface under different velocities. (A) WBCs (dots, blue line) and hGBM cells (squares, red line) capture efficiency at various flow velocities. (B) Captured mononuclear cells on the surface at the velocity of 0.5 mm/s. (C) Captured hGBM cells on the surface at the velocity of 4 mm/s. hGBM cells become flat, and pseudopods form. The scale bars are 50 μm.

of aptamers used during immobilization, the higher the number of cells that can be captured on the surface. We and others have previously published results where optimal conditions yield probe molecule density as high as 10^{12} molecules/cm^2.[34,35] It is envisioned that using probe DNA with the linker part of an aptamer would offer a better presentation of the aptamer to the solution-borne cells (CTCs or WBCs).[36]

However, the density of EGFR on the hGBM cell membrane can be roughly estimated by using the surface area to divide the total amount of EGFR.[22,23] It comes to be around 1 receptor/100 nm^2. The number of aptamers in the same area on the substrate is around 20−25. Although the receptor and aptamer have one-to-one binding, more aptamers undoubtedly can increase the odds of binding. In other words, with an optimal density of surface-bound aptamers, it is only the EGFR density on the cell membrane that is the most important factor in cell capture.

The capture efficiency was defined as the ratio of the number of captured cells to the total number of cells flowing through the whole channel. Bovine mononuclear cells were studied first. The capture efficiency values of mononuclear cells at 0.5, 1, 1.5, and 2 mm/s flow velocity were 53.64% (SD: 10.08%), 15.43% (SD: 6.53%), 1.38% (SD: 1.8%), and 0.62 (SD: 1.09%), respectively. The data is plotted in Figure 3A. Figure 3B shows the captured mononuclear cells on the surface at the velocity of 0.5 mm/s. The capture efficiency at 0.5 mm/s was seen to be much higher than the predicted value of adhesion probability (approximately 35%, Figure 2). However, the overall decreasing trend of the adhesion probability with increased flow velocity agrees qualitatively very well with the measured data. The deviations in the values between theory and experiments can be ascribed to the ideal setup used in the model, which assumed a uniform channel height, smooth surface, rigid cell, specific ligand−receptor binding, no-collision between cells, etc. At a lower velocity, especially in a low Reynolds number flow, cells could easily deviate from the flowing suspension and diffuse to the microfluidic channel bottom surface under the force of gravity.[37] As mentioned before, the diameter of mononuclear cells was around 6−8 μm, and very few cells were of the size 14 μm or more. The height of the channel (25 μm) was 2−3 times higher than the cell diameter. The cells could collide with the aptamer functionalized surface after traveling short distances in the flow, unlike hGBM cells, which were exposed to higher velocity. In our experiments, we did find the hGBM cell density at the rear end to be slightly higher than that at the front part, and that is why the standard deviation was slightly larger. This difference in density can be attributed to the relatively high flow rate that drove more hGBM cells to the lateral part before these came in contact with the surface.

The aptamer-EGFR binding process is instantaneous. Once they firmly bind together, the total binding force can be predicted using existing models.[27−29] On the basis of the model presented in ref 27, the single aptamer-EGFR binding force is around 8×10^{-6} dynes, and when the mononuclear cells firmly attach to the surface, the total binding force is around 0.06 dyn. This force is calculated by multiplying the contact area, the receptor density, and the single aptamer-EGFR binding force, assuming the cell radius to be 5 μm and maximum contact area of πr^2 (Table 1).

If we do not apply accelerated flow to the cells,[25] the washing speed could be estimated by Stokes' Law, and the washing speed should reach 17 m/s to wash off the attached cells. However, from our observations, the captured mononuclear cells can be eluted at a flow rate of 10 cm/s. Because of the lower EGFR density and the cellular properties, mononuclear cells cannot become flat to bind firmly and completely to the aptamer-functionalized surface.[24] Compared to the heights of captured

hGBM cells, which are less than 6 μm (measured with Zeiss LSM510 confocal microscope), the heights of the attached mononuclear cells do not decrease significantly. The other reason might be that some receptors may not bind with aptamers correctly or not bind at all. The situation also exists for hGBM cells (discussed later). In traditional approaches, the cells are incubated on aptamer- or antibody-functionalized surfaces, and then the surface is washed to elute nonspecifically bound cells. The major disadvantage of this method is that a higher washing speed is needed to elute these cells after these are firmly attached to the surface. The washing speed optimization is completely based on the experimental experience. However, in the microfluidic devices, the cell adhesion probability can be controlled by choosing a suitable flow velocity, toward higher efficiency and with a minimal amount of sample needed.

As depicted in Figure 3A, around 50% of mononuclear cells could be captured on the surface at 0.5 mm/s. We thus adopted 1, 2, 4, and 6 mm/s for hGBM cell isolation. The capture percentages of hGBM cells at 1, 2, 4, and 6 mm/s were 70.43% (SD, 15.67%; relative SD, 22.25%), 48.54% (SD, 12.95%; relative SD, 26.7%), 28.33% (SD, 9.37%; relative SD, 33%), and 15.44% (SD, 4.84%; relative SD, 31.35%), respectively. In this case, the capture efficiency was less than the predicted one at each velocity. The probable reason is that not all EGFRs bind to aptamers. If we examine the maximal values of capture percentage, it seems those values were close to the predicted ones. In the simulation, the cells are assumed to be initially attached to the surface, where the margination process before binding was not considered. The adhesion probability was the probability of the cells keeping adhered without being washed away at a given shear rate. However, in the experiments, the cells do marginate toward the bottom of the microchannel. The percentage of the cells attached at the bottom is the total number of adhered cells divided by total cells flushed in the test, which leads to a large deviation. For higher flow rate, the number of cells attached on the surface decreases significantly, which leads to a smaller deviation.

Also on the basis of the model of Bell, the total binding force is around 0.63 dyn if hGBM cells completely and firmly attach to the aptamer-functionalized surface.[27] The higher binding force indicates that the hGBM cells can more firmly attach to the surface, and the decreased cell height (less than 6 μm) further helps them from being washed-off under high flow velocity. When we use a 10 cm/s speed for cell elution, parts of the cell cannot resist high shear force, and we can find some cell fragments left on the surface. Figure 3C shows the captured hGBM cells at the velocity of 4 mm/s. When hGBM cells were firmly attached to the surface, the cells became flatter; the diameter of the cells also became bigger; and many pseudopodia were formed. Their appearance was quite different from that of mononuclear cells. This was consistent with the prior knowledge that the hGBM cells have strong activity when bound to an aptamer-functionalized surface and that they can change their shape arbitrarily.[24]

On the basis of the above results and analysis, a 2 mm/s flow was investigated to effectively separate the cell mixture of hGBM cells and mononuclear cells in a ratio of 1:1. Because not all hGBM cells can give clear fluorescence, we seeded cells on common glass slides and counted the total number of cells with and without fluorescence. We found that about 11.2% of the hGBM cells did not show any fluorescence. After separation and data calibration, the results showed surface-bound aptamers could selectively isolate and enrich a 1:1 mixture suspension

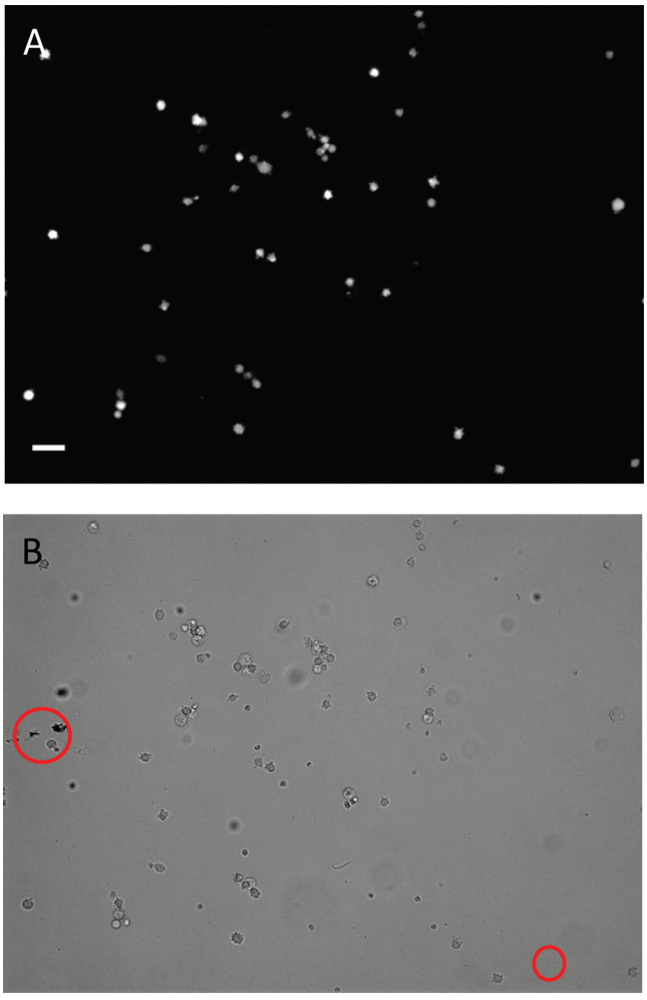

Figure 4. Experimental results of WBCs and hGBM cells captured on the anti-EGFR aptamer-functionalized surface from a 1:1 mixture. (A) and (B) are fluorescent and DIC images, respectively, from the same position. The circles in B indicate a few WBCs that were captured and cannot be seen in A. The scale bar is 50 μm.

ratio of mononuclear cells to hGBM cells to 1:42.67 on the surface (Figure 4). Mononuclear cells are circled in Figure 4. The results show that the aptamer-functionalized microfluidic channel can significantly improve the tumor cell isolation efficiency by optimizing the flow velocity.

CONCLUSION

A 25 μm high microfluidic channel functionalized with an anti-EGFR aptamer was used to study the effects of flow velocity on hGBM cells and bovine mononuclear cells capture efficiency. Very few mononuclear cells adhered to the aptamer-functionalized surface when the flow velocity was over 1.5 mm/s. On the contrary, 15.44% of EGFR-overexpressing hGBM cells could still be captured on the surface when the velocity reached 6 mm/s. We found at this height in the channel, a 2 mm/s flow rate could significantly facilitate cell mixture separation from 1:1 to 1:42.67. The analysis provides important insights into the design of microfluidic devices that use surface-tethered probes to capture cells. This can be useful toward improving efficiency of lab-on-chip approaches aimed at CTC isolation from peripheral blood.

AUTHOR INFORMATION

Corresponding Author
*E-mail: smiqbal@uta.edu.

ACKNOWLEDGMENT

We thank Laci Adolfo for help with manuscript preparation and Annas Javed for useful discussions. The aptamers were provided by Andrew D. Ellington at University of Texas at Austin, and tumor samples were provided by Robert Bachoo at University of Texas Southwestern Medical Center. This work was supported with NSF CAREER grant ECCS-0845669 (to S.M.I.). W.A. and Y.W. were partially supported with a fellowship from the Consortium for Nanomaterials for Aerospace Commerce and Technology (CONTACT) program, Rice University, Houston, TX, USA. Y.L. acknowledges support from the NSF grant CBET-1113040 and NIH grant EB009786.

REFERENCES

(1) Maheswaran, S.; Sequist, L. V.; Nagrath, S.; Ulkus, L.; Brannigan, B.; Collura, C. V.; Inserra, E.; Diederichs, S.; Iafrate, A. J.; Bell, D. W. *N. Engl. J. Med.* **2008**, *359*, 366–377.
(2) Paterlini-Brechot, P.; Benali, N. L. *Cancer Lett.* **2007**, *253*, 180–204.
(3) He, W.; Wang, H.; Hartmann, L. C.; Cheng, J. X.; Low, P. S. *Proc. Natl. Acad. Sci. U.S.A.* **2007**, *104*, 11760–11765.
(4) Huang, L. R.; Cox, E. C.; Austin, R. H.; Sturm, J. C. *Science* **2004**, *304*, 987–990.
(5) Bustin, S. A.; Gyselman, V. G.; Siddiqi, S.; Dorudi, S. *Int. J. Surg. Invest.* **2000**, *2*, 49–57.
(6) MacDonald, M. P.; Neale, S.; Paterson, L.; Richies, A.; Dholakia, K.; Spalding, G. C. *J. Biol. Regul. Homeostatic Agents* **2004**, *18*, 200–205.
(7) Lee, J. N.; Park, C.; Whitesides, G. M. *Anal. Chem.* **2003**, *75*, 6544–6554.
(8) Zieglschmid, V.; Hollmann, C.; Böher, O. *Crit. Rev. Clin. Lab. Sci.* **2005**, *42*, 155–196.
(9) Toner, M.; Irimia, D. *Annu. Rev. Biomed. Eng.* **2005**, *7*, 77–103.
(10) Adams, A. A.; Okagbare, P. I.; Feng, J.; Hupert, M. L.; Patterson, D.; Gottert, J.; McCarley, R. L.; Nikitopoulos, D.; Murphy, M. C.; Soper, S. A. *J. Am. Chem. Soc.* **2008**, *130*, 8633–8641.
(11) Nagrath, S.; Sequist, L. V.; Maheswaran, S.; Bell, D. W.; Irimia, D.; Ulkus, L.; Smith, M. R.; Kwak, E. L.; Digumarthy, S.; Muzikansky, A. *Nature* **2007**, *450*, 1235–1239.
(12) Dalle, F.; Lopez, J.; Caillot, D.; Cuisenier, B.; Ecarnot Laubriet, A.; Dumont, L.; Bonnin, A. *Eur. J. Clin. Microbiol. Infect. Dis.* **2002**, *21*, 130.
(13) Bunka, D. H. J.; Stockley, P. G. *Nat. Rev. Microbiol.* **2006**, *4*, 588–596.
(14) Farokhzad, O. C.; Jon, S.; Khademhosseini, A.; Tran, T. N. T.; LaVan, D. A.; Langer, R. *Cancer Res.* **2004**, *64*, 7668–7672.
(15) Chen, H. W.; Medley, C. D.; Sefah, K.; Shangguan, D.; Tang, Z.; Meng, L.; Smith, J. E.; Tan, W. *ChemMedChem* **2008**, *3*, 991–1001.
(16) Hoppe-Seyler, F.; Crnkovic-Mertens, I.; Tomai, E.; Butz, K. *Curr. Mol. Med.* **2004**, *4*, 529–538.
(17) Nagel-Wolfrum, K.; Buerger, C.; Wittig, I.; Butz, K.; Hoppe-Seyler, F.; Groner, B. *Mol. Cancer Res.* **2004**, *2*, 170–182.
(18) Phillips, J. A.; Xu, Y.; Xia, Z.; Fan, Z. H.; Tan, W. *Anal. Chem.* **2008**, *81*, 1033–1039.
(19) Mendelsohn, J. *Trans. Am. Clin. Climatol. Assoc.* **2004**, *115*, 249–254.
(20) Chakravarti, A.; Loeffler, J. S.; Dyson, N. J. *Cancer Res.* **2002**, *62*, 200.
(21) Franovic, A.; Gunaratnam, L.; Smith, K.; Robert, I.; Patten, D.; Lee, S. *Proc. Natl. Acad. Sci. U.S.A.* **2007**, *104*, 13092–13097.
(22) Carpenter, G.; Cohen, S. *Annu. Rev. Biochem.* **1979**, *48*, 193–216.
(23) Carpenter, G. *Mol. Cellul. Endocrinol.* **1983**, *31*, 1–19.
(24) Wan, Y.; Kim, Y.-t.; Li, N.; Cho, S. K.; Bachoo, R.; Ellington, A. D.; Iqbal, S. M. *Cancer Res.* **2010**, *70*, 9371–9380.
(25) Cheung, L. S. L.; Zheng, X.; Stopa, A.; Baygents, J. C.; Guzman, R.; Schroeder, J. A.; Heimark, R. L.; Zohar, Y. *Lab Chip* **2009**, *9*, 1721–1731.
(26) Krombach, F.; Müzing, S.; Allmeling, A. M.; Gerlach, J. T.; Behr, J.; Döger, M. *Environ. Health Perspect.* **1997**, *105*, 1261–1263.
(27) Bell, G. I. *Science* **1978**, *200*, 618–627.
(28) Kuo, S. C.; Lauffenburger, D. A. *Biophys. J.* **1993**, *65*, 2191–2200.
(29) Chang, K. C.; Hammer, D. A. *Biophys. J.* **1999**, *76*, 1280–1292.
(30) Decuzzi, P.; Ferrari, M. *Biomaterials* **2006**, *27*, 5307–5314.
(31) Shah, S.; Liu, Y.; Hu, W.; Gao, J. *J. Nanosci. Nanotechnol.* **2011**, *11*, 919–928.
(32) Iqbal, S. M.; Akin, D.; Bashir, R. *Nat. Nanotechnol.* **2007**, *2*, 243–248.
(33) Sequist, L. V.; Nagrath, S.; Toner, M.; Haber, D. A.; Lynch, T. J. *J. Thorac. Oncol.* **2009**, *4*, 281–283.
(34) Fuentes, M.; Mateo, C.; Garcia, L.; Tercero, J. C.; Guisan, J. M.; Fernandez-Lafuente, R. *Biomacromolecules* **2004**, *5*, 883–888.
(35) Peterson, A. W.; Heaton, R. J.; Georgiadis, R. M. *Nucleic Acids Res.* **2001**, *29*, 5163.
(36) Kemp, N. T.; Singh, N. K. *Langmuir* **2006**, *22*, 6222–6233.
(37) Staben, M. E.; Zinchenko, A. Z.; Davis, R. H. *Phys. Fluids* **2003**, *15*, 1711–1733.